



**HAL**  
open science

# Mesoscopic Controller for String Stability of Platoons With Disturbances

Marco Mirabilio, Alessio Iovine, Elena de Santis, Maria Domenica Di  
Benedetto, Giordano Pola

► **To cite this version:**

Marco Mirabilio, Alessio Iovine, Elena de Santis, Maria Domenica Di Benedetto, Giordano Pola. Mesoscopic Controller for String Stability of Platoons With Disturbances. IEEE Transactions on Control of Network Systems, 2022, 10.1109/TCNS.2022.3182038 . hal-03761237

**HAL Id: hal-03761237**

**<https://centralesupelec.hal.science/hal-03761237>**

Submitted on 29 Aug 2022

**HAL** is a multi-disciplinary open access archive for the deposit and dissemination of scientific research documents, whether they are published or not. The documents may come from teaching and research institutions in France or abroad, or from public or private research centers.

L'archive ouverte pluridisciplinaire **HAL**, est destinée au dépôt et à la diffusion de documents scientifiques de niveau recherche, publiés ou non, émanant des établissements d'enseignement et de recherche français ou étrangers, des laboratoires publics ou privés.

# Mesoscopic Controller for String Stability of Platoons with Disturbances

Marco Mirabilio, *Student Member, IEEE*, Alessio Iovine, *Member, IEEE*, Elena De Santis, *Senior Member, IEEE*, Maria Domenica Di Benedetto, *Life Fellow, IEEE*, Giordano Pola, *Senior Member, IEEE*

**Abstract**—This paper exploits macroscopic information for the control of autonomous vehicles in platoon formation in case of external disturbances. The use of such information leads to a smoother platooning. A mesoscopic controller is proposed, and Disturbance String Stability is proven through Input-to-State Stability (ISS) concepts. Simulations prove the efficacy of the proposed approach by showing its robustness with respect to the presence of perturbations acting on the platoon vehicles.

**Index Terms**—Vehicle platoon, String Stability, mesoscopic modeling, macroscopic information, Cooperative Adaptive Cruise Control, Input-to-State Stability, cascaded systems, mixed traffic

## I. INTRODUCTION

THE development of advanced traffic control technologies that enable vehicles to adapt their behaviour on the basis of real-time traffic conditions is a relevant subject in the framework of Smart Cities. Indeed, increasing traffic efficiency has a positive impact on our daily life, by reducing dangerous emissions and travel times thanks to less frequent and minor traffic congestion, car accidents and traffic jams [1], [2]. Different approaches have been proposed in literature, as for example the use of intelligent infrastructures and the displacement of autonomous vehicles, either in fully autonomous platoon formations or with a certain level of penetration rate among normal vehicles (see [3], [4], [5]). Although autonomous vehicles are not a new idea, only recent developments in the transportation industry and in communication technologies may allow their utilisation in real traffic situations. Indeed, nowadays Vehicle-to-Infrastructure (V2I) and Vehicle-to-Vehicle (V2V) communication technologies are a reality in smart transportation [6], enhancing the employment of the Adaptive Cruise Control (ACC). Then, it is important to define control policies that correctly exploit the shared data, enabling the autonomous vehicles to improve traffic throughput as well as to reduce perturbations propagation. In fact, interconnected autonomous vehicles can reduce stop-and-go waves propagation and traffic oscillations via the concepts of String Stability and Disturbance String Stability, based on the idea that the perturbations coming from a vehicle should not amplify backwards in the string [7], [8], [9].

Marco Mirabilio, Elena De Santis, Maria Domenica Di Benedetto and Giordano Pola are with the Department of Information Engineering, Computer Science and Mathematics, Center of Excellence DEWS, University of L'Aquila. (e-mail: marco.mirabilio@graduate.univaq.it, {elena.desantis, mariadomenica.dibenedetto, giordano.pola}@univaq.it)

Alessio Iovine is with the Laboratory of Signal and Systems (L2S), Centre National de la Recherche Scientifique (CNRS), CentraleSupélec, Paris-Saclay University, 3, rue Joliot-Curie, 91192 Gif-sur-Yvette, France. E-mail: alessio.iovine@l2s.centralesupelec.fr

The present work is based on the framework developed in [10] and [11], and extends it to the case where disturbances act on each vehicle. A platoon of autonomous vehicles is considered, and a controller implementing a variable spacing policy exploiting macroscopic information is proposed. In the case of vehicular platooning, disturbances may be due to reference speed variation, external inputs, unmodeled dynamics, and the sharing of corrupted or inexact information. For example, the presence of communication delays not properly compensated can propagate through the string inexact information that acts as a disturbance. Moreover, also the presence of human driven vehicles in a mixed traffic scenario can be a source of disturbances for the autonomous vehicles. Then, we illustrate how the same proposed framework can be exploited to describe the presence of human driven vehicles as a Disturbance String Stability problem from an autonomous vehicle point of view. The vehicles are assumed to be equipped with a communication technology supporting either V2V or V2I, or both, enabling them to exchange information. Each vehicle is considered either to correctly measure distance, speed and acceleration of its predecessor, using for example radar and LIDAR, or to receive them via V2V or V2I. The macroscopic information can be computed in a Smart City framework either from the whole platoon via inter-vehicular communication [12] or from the road infrastructure via the use of technologies as inductive loop detectors, video detection systems, infra-red tracking systems etc. [13]. In real scenarios, the estimation of the needed global quantities (e.g. inter-vehicular distance mean and variance) is not error-free, leading to unknown disturbances acting on the vehicles exploiting macroscopic information. Then, the Disturbance String Stability analysis framework suggested in the present paper targets to ensure platoon stability with respect to those disturbances. A thorough analysis about the possible methodologies for computing/estimating the global variables of interest is out of the scope of this paper, as it depends on a number of factors, including the communication technology adopted. Our utilisation of macroscopic information that is embedded in few variables, for example distance or speed difference mean and variance, replaces the need for sharing some microscopic variables among the whole platoon, e.g. the leading vehicle acceleration or its desired speed (see [9], [14] and [15]). Consequently, no direct communication between the first vehicle and the others is required, except for its immediate follower. It also results in a complexity reduction of both the considered interconnected framework and the system modeling without reducing the level of available information, as the whole set



$v_{\max}, v_{\max} \in \mathbb{R}^+, \forall i \in \mathcal{I}_N^0$ . Then, we define the state of the  $i$ -th vehicle as

$$x_i = [p_i \ v_i]^T. \quad (1)$$

The corresponding dynamical system is obtained by ignoring both reaction time delays and communication time delays [9], [24], [25], [3]:

$$\dot{x}_i = \begin{bmatrix} \dot{p}_i \\ \dot{v}_i \end{bmatrix} = \begin{bmatrix} v_i \\ u_i + d_i \end{bmatrix}, \quad i \in \mathcal{I}_N^0, \quad (2)$$

where  $|u_i| \leq u_{\max}, u_{\max} \in \mathbb{R}^+$ , is the control input of the  $i$ -th vehicle, corresponding to the acceleration. Although the double integrator model assumes instantaneous actuation, that is never the case in practice, it is classically used to analyse heterogeneous platoons [26], i.e. platoons composed by non identical vehicles. In order to describe inter-vehicular interactions, we adopt the leader-follower model (see [27]), with respect to we derive a global description of the platoon. For the derived model to include vehicle  $i = 0$ , we consider the presence of a virtual leader,  $i = -1$ , that precedes the entire platoon, with dynamical model

$$\dot{x}_{-1} = \begin{bmatrix} \dot{p}_{-1} \\ \dot{v}_{-1} \end{bmatrix} = \begin{bmatrix} v_{-1} \\ u_{-1} + d_{-1} \end{bmatrix} \quad (3)$$

where  $d_{-1}(t) = 0 \forall t \geq 0$ . Then, the state of each car-following situation between vehicle  $i - 1$  and  $i$  is defined as

$$\chi_i = x_i - x_{i-1} = \begin{bmatrix} \Delta p_i \\ \Delta v_i \end{bmatrix} = \begin{bmatrix} p_i - p_{i-1} \\ v_i - v_{i-1} \end{bmatrix}, \quad i \in \mathcal{I}_N^0. \quad (4)$$

The resulting microscopic dynamical model of the  $i$ -th car-following pair is:

$$\dot{\chi}_i = \begin{bmatrix} \Delta \dot{p}_i \\ \Delta \dot{v}_i \end{bmatrix} = \begin{bmatrix} \Delta v_i \\ u_i - u_{i-1} + d_i - d_{i-1} \end{bmatrix}, \quad i \in \mathcal{I}_N^0. \quad (5)$$

From (5), we observe that each car-following pair is affected by the disturbances acting on both the vehicles of the pair. This means that their contribution can either nullify or strengthen each other action. In order to shrink the notation, we define the constant vector  $c_d = [1 \ -1]$  and the lumped disturbance term  $\bar{d}_i = [d_i \ d_{i-1}]^T$ .

*Remark 1:* The presence of smart infrastructure sending traffic signals is not directly considered in the current modeling. However, the virtual vehicle's speed  $v_{-1}$  can be considered as the reference speed of  $i = 0$ , which can be either set by the smart infrastructure (e.g. smart intersections) or communicated by other interconnected vehicles.

To define the equilibrium point of the platoon, we consider the constant speed hypothesis for the virtual leader  $i = -1$  (see [27] and [28]) and the nominal case with no disturbances. If  $\bar{v} > 0$  is a constant speed, then  $p_{-1}(t) = \bar{v} \cdot t$ ,  $v_{-1}(t) = \bar{v}$ ,  $u_{-1}(t) = 0$ ,  $\forall t \geq 0$ . Assuming that  $\Delta \bar{p} > 0$  is the desired inter-vehicular distance at steady-state condition, and that  $\Delta p_0(t) = -\Delta \bar{p} \ \forall t \geq 0$ , then the equilibrium point for the  $i$ -th system of dynamics (5) corresponds to the case where all the vehicles have the same speed and are at the same distance:

$$\chi_{e,i} = \bar{\chi} = [-\Delta \bar{p} \ 0]^T, \quad \forall i \in \mathcal{I}_N^0. \quad (6)$$

Since the state vector (4) is defined with respect to the follower vehicle, then distance  $\Delta p_i$  and relative speed  $\Delta v_i$  have opposite sign. For this reason, the equilibrium distance in (6) is  $-\Delta \bar{p} < 0$ . From the platoon point of view, we define the lumped state and the lumped equilibrium point for  $u_{-1} = 0$  respectively as  $\chi = [\chi_0^T \ \chi_1^T \ \dots \ \chi_N^T]^T$  and  $\chi_e = [\chi_{e,0}^T \ \chi_{e,1}^T \ \dots \ \chi_{e,N}^T]^T = [\bar{\chi}^T \ \bar{\chi}^T \ \dots \ \bar{\chi}^T]^T$ .

### B. Problem formulation

As in the framework presented in [10] and [11], we consider a variable spacing policy among the several ones presented in the literature (see [14], [29]). The classical definition of variable spacing policy is such that if a constant time headway is maintained between two consecutive vehicles, then the inter-vehicular distance increases proportionally with respect to it. Differently, our objective is to vary the desired distance during the transient of the platoon system, and to reach a predefined constant distance when the vehicles are in a steady-state condition. To this purpose, we define the following *mesoscopic spacing policy*:

$$\Delta p_i^r(t) = -\Delta \bar{p} - \rho_i^M(t), \quad t \geq 0, \quad (7)$$

where  $\Delta \bar{p}$  is a constant inter-vehicular distance, and  $\rho_i^M$  is a function describing the macroscopic information related to the states of the platoon vehicles.

The objective of this paper is to develop dynamic controllers in the form of

$$\begin{cases} \dot{\rho}_i = \omega_i(\rho_i, \chi_i, \chi_{i-1}, \dots, \chi_0, \chi_{e,i}) \\ u_i = h_i(\rho_i, \chi_i, \chi_{i-1}, \dots, \chi_0, \chi_{e,i}, u_{i-1}) \end{cases} \quad (8)$$

for the asymptotic tracking of the desired distance (7). In (8),  $\rho_i \in \mathbb{R}^r$ ,  $r > 0$ , is the state of the dynamic controller;  $\omega_i : \mathbb{R}^r \times \underbrace{\mathbb{R}^2 \times \dots \times \mathbb{R}^2}_{i+1 \text{ times}} \times \mathbb{R}^2 \rightarrow \mathbb{R}^r$  is the vector field

describing the evolution of the dynamic system;  $h_i : \mathbb{R}^r \times \underbrace{\mathbb{R}^2 \times \dots \times \mathbb{R}^2}_{i+1 \text{ times}} \times \mathbb{R}^2 \times \mathbb{R} \rightarrow \mathbb{R}^r$  is the output function used to

compute the control input  $u_i$ ;  $\chi_i, \chi_{i-1}, \dots, \chi_0, \chi_{e,i}, u_{i-1}$  are the inputs of the system. In the sequel, we denote with  $P_{cl}$  the resulting closed-loop system, and we define the extended state vector  $\hat{\chi}_i$  and the corresponding equilibrium point  $\hat{\chi}_{e,i}$  for the  $i$ -th vehicle of the platoon as

$$\hat{\chi}_i = [\chi_i^T \ \rho_i^T]^T, \quad \hat{\chi}_{e,i} = [\bar{\chi}^T \ 0_r^T]^T, \quad \forall i \in \mathcal{I}_N^0, \quad (9)$$

where  $0_r \in \mathbb{R}^r$  is a null column vector. We now recall the definitions of String Stability, Asymptotic String Stability and Disturbance String Stability from [7], [10] and [15].

*Definition 1:* (String Stability) The equilibrium  $\hat{\chi}_{e,i}, i \in \mathcal{I}_N^0$ , of  $P_{cl}$  is said to be String Stable if, for any  $\epsilon > 0$ , there exists  $\delta > 0$  such that, for all  $N \in \mathbb{N}$ , for all  $t \geq 0$ ,

$$\max_{i \in \mathcal{I}_N^0} |\hat{\chi}_i(0) - \hat{\chi}_{e,i}| < \delta \Rightarrow \max_{i \in \mathcal{I}_N^0} |\hat{\chi}_i(t) - \hat{\chi}_{e,i}| < \epsilon. \quad (10)$$

*Definition 2:* (Asymptotic String Stability) The equilibrium  $\hat{\chi}_{e,i}, i \in \mathcal{I}_N^0$ , of  $P_{cl}$  is said to be Asymptotically String Stable if it is String Stable and, for all  $N \in \mathbb{N}$ ,

$$\lim_{t \rightarrow \infty} |\hat{\chi}_i(t) - \hat{\chi}_{e,i}| = 0, \quad \forall i \in \mathcal{I}_N^0. \quad (11)$$

**Definition 3:** (Disturbance String Stability) The equilibrium  $\hat{\chi}_{e,i}$ ,  $i \in \mathcal{I}_N^0$ , of  $P_{cl}$  is said to be Disturbance String Stable if there exist functions  $\beta_d$  of class  $\mathcal{KL}$  and  $\sigma_d$  of class  $\mathcal{K}_\infty$  and constants  $\delta > 0$ ,  $\delta_d > 0$ , such that, for any initial condition  $\hat{\chi}_i(0)$  and disturbance  $\bar{d}_i$  satisfying

$$\max_{i \in \mathcal{I}_N^0} |\hat{\chi}_i(0) - \hat{\chi}_{e,i}| < \delta, \quad \max_{i \in \mathcal{I}_N^0} |\bar{d}_i(\cdot)|_\infty^{[0,t]} < \delta_d \quad (12)$$

the solution  $\hat{\chi}_i(t)$  exists for all  $t \geq 0$  and satisfies

$$\begin{aligned} \max_{i \in \mathcal{I}_N^0} |\hat{\chi}_i(t) - \hat{\chi}_{e,i}| \leq & \beta_d \left( \max_{i \in \mathcal{I}_N^0} |\hat{\chi}_i(0) - \hat{\chi}_{e,i}|, t \right) \\ & + \sigma_d \left( \max_{i \in \mathcal{I}_N^0} |\bar{d}_i(\cdot)|_\infty^{[0,t]} \right) \quad \forall N \in \mathbb{N}. \end{aligned} \quad (13)$$

The aim of this paper is not only to ensure tracking of the reference distance (7), but also to ensure Disturbance String Stability of the closed-loop system  $P_{cl}$  as in the definition above.

### III. DISTURBANCE STRING STABILITY ANALYSIS

In this section, we investigate Disturbance String Stability of a general class of cascaded interconnected systems. We consider that each vehicle takes as input  $u_i$  the output signal of (8). Then, we consider the extended state  $\hat{\chi}_i$  and the corresponding equilibrium point  $\hat{\chi}_{e,i}$  in (9) describing the  $i$ -th car-following pair closed-loop system. Let  $\tilde{\chi}_i = \hat{\chi}_i - \hat{\chi}_{e,i}$ , then the closed-loop dynamics of the platoon is described by the following class of cascaded interconnected systems

$$\begin{aligned} \dot{\tilde{\chi}}_0 &= f_{cl}(\tilde{\chi}_0, \bar{d}_0), \\ \dot{\tilde{\chi}}_i &= f_{cl}(\tilde{\chi}_i, \bar{d}_i) + g_{cl,i}(\tilde{\chi}_{i-1}, \dots, \tilde{\chi}_0), \quad \forall i \in \mathcal{I}_N, \end{aligned} \quad (14)$$

where  $f_{cl} : \mathbb{R}^{2+r} \times \mathbb{R}^2 \rightarrow \mathbb{R}^{2+r}$  is the vector field describing the dynamics of the  $i$ -th isolated subsystem, and  $g_{cl,i} : \underbrace{\mathbb{R}^{2+r} \times \dots \times \mathbb{R}^{2+r}}_{i \text{ times}} \rightarrow \mathbb{R}^{2+r}$  is the interconnection term. For the first vehicle, we assume that  $g_{cl,0}(\tilde{\chi}_{-1}) = 0$ . Moreover,  $f_{cl}(0, 0) = 0$  and  $g_{cl,i}(0, 0, \dots, 0) = 0$ .

**Theorem 1:** Consider the autonomous system in (14). If there exist functions  $\beta$  of class  $\mathcal{KL}$  and  $\gamma, \sigma$  of class  $\mathcal{K}_\infty$ , such that for each  $i \in \mathcal{I}_N^0$

$$\begin{aligned} |\tilde{\chi}_i(t)| \leq & \beta(|\tilde{\chi}_i(0)|, t) + \gamma \left( \max_{j=0, \dots, i-1} |\tilde{\chi}_j(\cdot)|_\infty^{[0,t]} \right) \\ & + \sigma(|\bar{d}_i(\cdot)|_\infty^{[0,t]}) \end{aligned} \quad (15)$$

$\forall t \geq 0$  and  $\gamma(s) \leq \tilde{\gamma}s$ , for  $s \geq 0$  and  $\tilde{\gamma} \in (0, 1)$ , then the interconnected system is Disturbance String Stable.

*Proof.* See Appendix A.  $\square$

**Remark 2:** Note that the result above is quite general since it only depends on the structure of the cascaded interconnected system (14). Therefore, it can be applied not only to platoons of vehicles, but to any interconnected system showing the same form.

**Remark 3:** Differently from the results provided in [11], that are based on the use of composite Lyapunov functions, here the proof of Theorem 1 is based on exploiting the properties of  $\mathcal{KL}$  and  $\mathcal{K}_\infty$  functions. Moreover, the proof takes into account the

presence of disturbances acting on the system. In the special case of no disturbances, Theorem 1 requires weaker conditions than the ones in [11, Theorem 1] on the interconnection terms  $g_{cl,i}$ , where the bound  $|g_{cl,i}(\tilde{\chi}_{i-1}, \dots, \tilde{\chi}_0)| \leq \sum_{j=0}^{i-1} k_{ij} |\tilde{\chi}_j|$ ,  $k_{ij} \in \mathbb{R}^+$ ,  $\forall i \in \mathcal{I}_N^0$ , is required for the Asymptotic String Stability of the platoon.

### IV. CONTROL DESIGN AND THE MIXED TRAFFIC CASE

In this section, we propose a macroscopic control law for tracking the desired distance (7), and we prove that the obtained closed-loop dynamics of the platoon can be described by the class of cascaded interconnected systems (14). Then, we prove that Disturbance String Stability is ensured by Theorem 1. Finally, we describe how the mixed traffic scenario can be modeled as a Disturbance String Stability problem for the autonomous vehicle.

#### A. Macroscopic information

The macroscopic information is supposed to be shared either by the vehicles via V2V, or by the infrastructure via V2I. The goal is to define proper functions that allow to reduce the amount of the shared data, without reducing the level of available information. To this purpose, we consider mean and variance of the inter-vehicular distance and speed difference as the macroscopic variables shared to the platoon. Given the generic vehicle  $i \in \mathcal{I}_N^0$ ,  $\mu_{l,i}$  and  $\sigma_{l,i}^2$  denote the inter-vehicular distance ( $l = \Delta p$ ) and speed error ( $l = \Delta v$ ) mean and variance, respectively, computed from vehicle 0 to vehicle  $i$ , and are defined as

$$\mu_{l,i} = \frac{1}{i+1} \sum_{j=0}^i l_j, \quad \sigma_{l,i}^2 = \frac{1}{i+1} \sum_{j=0}^i (l_j - \mu_{l,i})^2, \quad (16)$$

where  $l \in \{\Delta p, \Delta v\}$ . With the scope to provide the  $i$ -th vehicle with the macroscopic information embedded in  $\mu_{l,i}$  and  $\sigma_{l,i}^2$ ,  $i \in \mathcal{I}_N^0$ , we define the distance macroscopic function  $\psi_{\Delta p}^i : \mathbb{R} \times \mathbb{R}^+ \rightarrow \mathbb{R}$ , and the speed tracking error macroscopic function  $\psi_{\Delta v}^i : \mathbb{R} \times \mathbb{R}^+ \rightarrow \mathbb{R}$ . Being computed over the mean and the variance (16), functions  $\psi_l^i$  represent the state of the vehicles ahead. In particular,  $\psi_{\Delta p}^i = \psi_{\Delta v}^i = 0$  means that the vehicles up to the  $i$ -th one have no oscillations. As in [11], we consider the macroscopic functions given in the following:

$$\psi_l^i = \gamma_l \text{sign}(\mu_{l,i} - \bar{\chi}_l) \sqrt{\sigma_{l,i}^2}, \quad l \in \{\Delta p, \Delta v\}, \quad (17)$$

where  $\bar{\chi}_{\Delta p} = -\Delta \bar{p}$ ,  $\bar{\chi}_{\Delta v} = 0$  and  $\gamma_{\Delta p}, \gamma_{\Delta v} > 0$  are constant parameters. The direct outcome of embedding macroscopic information in (16) in (17) is that we avoid to consider the whole set of leader-follower states, i.e.  $\chi$ , without reducing the level of available information. Functions  $\psi_l^i$  are later exploited to let the controller state  $\rho_i$  with dynamics (8) evolve with respect to the macroscopic information of the platoon (see Section IV-B).

**Remark 4:** We remark that mean and variance of the microscopic quantities are related to traffic macroscopic variables such as traffic density that is the inverse of inter-vehicular mean distance [30, ch. 2, p. 26]. Moreover, there exist several diagrams describing the interconnection between local and global quantities, as the speed-density diagram [16, ch. 4].

## B. Mesoscopic Control Law

In order to achieve Disturbance String Stability of the platoon, we propose the following dynamical system describing the interconnection of the controller state with the macroscopic information:

$$\begin{cases} \dot{\rho}_i = \Lambda \rho_i + G_\rho^\psi \psi^{i-1} + G_\rho^e e_i \\ \rho_i(0) = 0 \end{cases} \quad (18)$$

where  $\rho_i = [\rho_{1,i} \ \rho_{2,i}]^T$ ,  $\psi^i = [\psi_{\Delta p}^i \ \psi_{\Delta v}^i]^T$ ,  $e_i = \chi_i - \chi_{e,i}$ , and

$$\Lambda = \begin{bmatrix} -\lambda_1 & 1 \\ 0 & -\lambda_2 \end{bmatrix}, G_\rho^\psi = \begin{bmatrix} 0 & 0 \\ a & b \end{bmatrix}, G_\rho^e = \begin{bmatrix} w & 0 \\ 0 & 0 \end{bmatrix}.$$

The diagonal entries of matrix  $\Lambda$  are  $\lambda_1, \lambda_2 > 0$ , so that  $\rho_i \rightarrow 0$  as  $\psi_{\Delta p}^i \rightarrow 0$ ,  $\psi_{\Delta v}^i \rightarrow 0$ ,  $\Delta p_i \rightarrow -\Delta \bar{p}$  and  $\Delta v_i \rightarrow 0$ ;  $G_\rho^\psi$  is the input matrix associated to the macroscopic functions, with parameters  $a, b \geq 0$ ;  $G_\rho^e \in \mathbb{R}^{r \times 2}$  is the input matrix associated to the local leader-follower state, with  $w \in \mathbb{R}$ . As a consequence, it is possible to vary the controller response with respect to variations of the macroscopic variables and the microscopic ones through an appropriate choice of  $\Lambda$  as well as of the elements of matrices  $G_\rho^\psi$  and  $G_\rho^e$ . Differently from [10] and [11], the presence of  $G_\rho^e$  in (18) allows to weight the local information over the macroscopic one. The superscript  $i-1$  denotes that for the  $i$ -th system the macroscopic information from vehicle 0 to the preceding one  $i-1$  is exploited. For vehicle  $i=0$ ,  $\psi_{\Delta p}^{-1} = \psi_{\Delta v}^{-1} = 0$  is set. Since  $\rho_{1,i}$  contains both microscopic and macroscopic information, we set  $\rho_i^M = \rho_{1,i}$ . The control law  $u_i$  is derived with respect to the open-loop dynamics describing the evolution of the extended state  $\hat{\chi}_i$  defined in (9). The resulting dynamical system is obtained by coupling the dynamics of the  $i$ -th car-following pair (5) and the controller dynamics (18). Then, the following control law letting the vehicle track the desired reference distance (7) is derived via backstepping method:

$$\begin{aligned} u_i &= u_{i-1} - (1 + \lambda_1 K_{\Delta p})(\Delta p_i + \Delta \bar{p} + \rho_{1,i}) \\ &\quad + \lambda_1(-\lambda_1 \rho_{1,i} + \rho_{2,i}) + \lambda_2 \rho_{2,i} - \psi_{a,b}^{i-1} \\ &\quad - K_{\Delta v}(\Delta v_i - \lambda_1 \rho_{1,i} + \rho_{2,i}), \end{aligned} \quad (19)$$

where  $w = -K_{\Delta p}$ ,  $K_{\Delta p}, K_{\Delta v} > 0$  are control gains equal for each  $i \in \mathcal{I}_N^0$ , and  $\psi_{a,b}^i = a\psi_{\Delta p}^i + b\psi_{\Delta v}^i$ . The resulting closed-loop dynamical system is

$$\dot{\hat{\chi}}_i = \begin{bmatrix} \Delta v_i \\ (*) + c_d \bar{d}_i \\ -\lambda_1 \rho_{1,i} + \rho_{2,i} - K_{\Delta p}(\Delta p_i + \Delta \bar{p} + \rho_{1,i}) \\ -\lambda_2 \rho_{2,i} + \psi_{a,b}^{i-1} \end{bmatrix} \quad (20)$$

with

$$\begin{aligned} (*) &= -(1 + \lambda_1 K_{\Delta p})(\Delta p_i + \Delta \bar{p} + \rho_{1,i}) + \lambda_2 \rho_{2,i} - \psi_{a,b}^{i-1} \\ &\quad + \lambda_1(-\lambda_1 \rho_{1,i} + \rho_{2,i}) - K_{\Delta v}(\Delta v_i - \lambda_1 \rho_{1,i} + \rho_{2,i}). \end{aligned}$$

Clearly, system (20) is in the form (14), and the following result can be proved:

*Theorem 2:* If  $K_{\Delta p}, K_{\Delta v}, \lambda_1, \lambda_2 > 0$ , then there exist functions  $\beta$  of class  $\mathcal{KL}$  and  $\gamma, \sigma$  of class  $\mathcal{K}_\infty$  such that system (20) verifies inequality (15), with  $\gamma(s) = \tilde{\gamma}s$ . Moreover, there

exist  $a$  and  $b$  in (18) such that  $\tilde{\gamma} \in (0, 1)$ , thus ensuring the Disturbance String Stability of the platoon.

*Proof.* See Appendix B.  $\square$

The use of macroscopic information, embedded in the macroscopic function  $\rho_i^M$ , allows establishing an interconnection between vehicle  $i$  and the vehicles ahead, here represented by  $\tilde{\gamma}$ . Then, to correctly size the contribution of the global information to stabilize the platoon, an appropriate choice of the controller parameters  $a$  and  $b$  is needed. We remark that this choice is very important to bound the interconnection intensity, as  $\tilde{\gamma} \in (0, 1)$  must be guaranteed.

## C. Mixed Traffic as Disturbance String Stability problem

In this section, we describe how the mixed traffic scenario can be modeled as a Disturbance String Stability problem for the autonomous vehicle. To this purpose, let us define the set of human-driven vehicles as  $\mathcal{I}_{HD} \subset \mathcal{I}_N^0$ , and the set of autonomous vehicles as  $\mathcal{I}_{AV} = \mathcal{I}_N^0 \setminus \mathcal{I}_{HD}$ . We assume the non-autonomous vehicles  $j \in \mathcal{I}_{HD}$  to not send and receive any information to and from the platoon. We suppose that each vehicle  $i \in \mathcal{I}_{AV}$  applies a disturbance string stable control law given by the dynamic controller in (8), where the control input is computed through the output function  $h_i(\rho_i, \chi, \chi_e, u_{i-1})$ . Since the leader-follower model in (5) can also represent the interaction between the two typologies of vehicles as well as the interactions between two consecutive human driven vehicles, we consider a control input  $u_j^{HD} = h_{HD}(\chi_j)$  for each  $j \in \mathcal{I}_{HD}$  that is characterised in a general form according to the ad hoc considered model (Intelligent Driver Model, Optimal Velocity Model, etc) [31]. Then,  $u_j^{HD}$  is the human driver control policy based only on local information. As in [32], we assume that the human-driven vehicles try to maintain their equilibrium point. Although in a mixed platoon there may be a number of permutations, we focus on the case where the human driven vehicle  $j$  precedes the autonomous one  $j+1$ :

$$\dot{\chi}_{j+1} = \begin{bmatrix} \Delta v_{j+1} \\ u_{j+1} - u_j^{HD} + d_{j+1} - d_j^{ext} \end{bmatrix}, \quad (21)$$

where  $d_j^{ext}$  is a possible external disturbance acting on the non autonomous vehicle. Since human driven vehicles do not send any information, then the control input  $u_j^{HD}$  cannot be appropriately compensated by the follower  $j+1$ , resulting in an additional disturbance acting on the  $j+1$ -th leader-follower state. Defining  $d_j = d_j^{ext} + u_j^{HD}$ , we get

$$\dot{\chi}_{j+1} = \begin{bmatrix} \Delta v_{j+1} \\ u_{j+1} + d_{j+1} - d_j \end{bmatrix}. \quad (22)$$

As long as the bounds of disturbance term  $\bar{d}_{j+1} = [d_{j+1} \ d_j]^T$  respects the bounds in Definition 3, the system (22) describes the interaction among a non autonomous leader and an autonomous follower. Without loss of generality, we can consider  $u_j = 0 \ \forall t \geq 0$ . As it is shown by the on-field experiments results reported in [33], [34] and [35], the human behaviour can cause the triggering of stop-and-go waves. Then, in the mixed traffic scenario a boundedness problem of the control input  $u_j^{HD}$  can arise in case of several consecutive non autonomous vehicles. Consequently, it is not possible to

ensure conditions (10) and (11) in Definitions 1 and 2, or (13) in Definition 3 if disturbances act on the platoon, for each  $N \in \mathbb{N}$ . In order to deal with the mixed traffic scenario, we need to relax the classical notion of String Stability and refer to a weaker definition that allows for the presence of String Instable vehicles in the platoon, at the cost of losing the uniformity with respect to the platoon length (see [36]). On this basis, let us consider  $M$  consecutive human driven vehicles preceding the autonomous one, that for simplicity we assume to be indexed by  $\mathcal{I}_{HD} = \{0, \dots, M-1\}$ . We define  $\chi_{HD,e}$  as the equilibrium point of the vehicles applying the control law  $h_{HD}(\chi_j)$ , and  $\tilde{\chi}_{HD,j} = \chi_{e,j} - \chi_{HD,e}$ . When considering the human driver model, we remark that the equilibrium  $\chi_{HD,e}$  varies with respect to the current speed. The closed-loop dynamics is represented by:

$$\dot{\tilde{\chi}}_{HD,j} = f_{cl}^{HD}(\tilde{\chi}_{HD,j}, \tilde{\chi}_{HD,j-1}, \bar{d}_j), \quad \forall j \in \mathcal{I}_{HD}. \quad (23)$$

Although we consider system (23) to be String Instable, it is possible to prove its local stability (see [32]). Therefore, there exist functions  $\beta_{HD} \in \mathcal{KL}$  and  $\sigma_{HD} \in \mathcal{K}_\infty$  such that,  $\forall t \geq 0$ ,

$$|\tilde{\chi}_{HD,j}(t)| \leq \beta_{HD}(|\tilde{\chi}_{HD,j}(0)|, t) + \tilde{\gamma}_{HD} |\tilde{\chi}_{HD,j}(\cdot)|_\infty^{[0,t]} + \sigma_{HD}(|\bar{d}_j(\cdot)|_\infty^{[0,t]}), \quad \forall j \in \mathcal{I}_{HD}, \quad (24)$$

with  $\tilde{\gamma}_{HD} > 1$ . In accordance with the forward recursive procedure adopted in the proof of Theorem 1, by setting  $t = 0$  we compute the following maximal bound for the human driven vehicles trajectories  $\forall j \in \mathcal{I}_{HD}$ :

$$|\tilde{\chi}_{HD,j}(t)| \leq \frac{1 - \tilde{\gamma}_{HD}^j}{1 - \tilde{\gamma}_{HD}} \beta_{HD} \left( \max_{l \in \mathcal{I}_{HD}} |\tilde{\chi}_{HD,l}(0)|, 0 \right) + \frac{1 - \tilde{\gamma}_{HD}^j}{1 - \tilde{\gamma}_{HD}} \sigma_{HD} \left( \max_{l \in \mathcal{I}_{HD}} |\bar{d}_l(\cdot)|_\infty^{[0,t]} \right), \quad (25)$$

where the multiplicative factor  $\frac{1 - \tilde{\gamma}_{HD}^j}{1 - \tilde{\gamma}_{HD}}$  is the result of the corresponding finite geometric series. From (25), we observe that the trajectory error norm bound increase while moving toward the tail of the string of human driven vehicles. This means that an oscillation originated from the head vehicles can cause the trajectory of the tail ones to move in a greater neighborhood of the equilibrium point, causing, in turn, the perturbation amplification. Since we are able to define trajectory bounds for each leader-follower state, either when considering the case of autonomous or non autonomous follower vehicle, we can compute the related bound for the applied control input. It is clear that for the disturbance string stable policy in (19) this bound does not depend on the platoon length. On the contrary, for the human driven vehicles the control input bound increases with respect to the platoon length. As a consequence, Disturbance String Stability of (22) can not be ensured for arbitrary  $M$ . We can conclude that there exists a  $\bar{M}$  such that, for  $M > \bar{M}$ , the autonomous vehicle is not able to handle the perturbations due to the string of human driven vehicles.

## V. SIMULATIONS

In this section, we describe simulation results to validate the proposed control strategy. In order to test the robustness of the controller, we performed simulations in three different

scenarios. The first scenario refers to a full autonomous platoon of  $N + 1$  vehicles tracking a variable reference speed supposed to be either set by the smart infrastructure (e.g. smart intersections) or communicated by other interconnected vehicles (Figures 2a, 2b and 2c). The second scenario refers to the mixed traffic case, in which the  $N + 1$  vehicles are both autonomous and human driven (Figures 3a, 3b, 3c and 3d). In the third scenario, we consider the departure and stop at the traffic light of a platoon of autonomous vehicle (Figures 4a, 4b and 4c). The color legend adopted is the same for each figure. Each line represents the trajectory of the leader-follower variable to which the figure refers. Then, the color scale from the blue tint to the light green one represents the vehicles of the platoon, from the head vehicles to the tail ones, respectively. In the simulations, we consider the autonomous vehicles having non-ideal actuator dynamics with delay  $\tau = 0.2$  s; such unmodeled dynamics results to be a perturbation on the commanded acceleration or brake action. Moreover, since each autonomous vehicle communicates its control input  $u_i$  to the following autonomous vehicle, if it is present, the before mentioned unmodeled actuator delay has the effect to corrupt the shared data, resulting in a perturbation for the  $i + 1$ -th vehicle. Then, it allows to test the robustness of the proposed controller with respect to realistic unmodeled dynamics. We consider the vehicle speed such that  $0 < v_i \leq 40$  m/s and the acceleration such that  $|u_i| \leq 4$  m/s<sup>2</sup>.

TABLE I: The control parameters: full autonomous platoon.

Parameter	Value	Parameter	Value	Parameter	Value
$K_{\Delta p}$	3	$K_{\Delta v}$	4	$\Upsilon$	0.99
$\lambda_1$	2	$\lambda_2$	1.5	$a$	0.6
$b$	0.6	$\gamma_{\Delta p}, \gamma_{\Delta v}$	0.5	$\tilde{\gamma}$	0.49

TABLE II: The control parameters: mixed traffic.

Parameter	Value	Parameter	Value	Parameter	Value
$K_{\Delta p}$	3	$K_{\Delta v}$	4	$\Upsilon$	0.99
$\lambda_1$	2	$\lambda_2$	1.5	$a$	1.2
$b$	0	$\gamma_{\Delta p}, \gamma_{\Delta v}$	0.5	$\tilde{\gamma}$	0.49

TABLE III: The control parameters: traffic light scenario.

Parameter	Value	Parameter	Value	Parameter	Value
$K_{\Delta p}$	1.4	$K_{\Delta v}$	1.4	$\Upsilon$	0.99
$\lambda_1$	1.1	$\lambda_2$	1.2	$a$	0.4
$b$	0.4	$\gamma_{\Delta p}, \gamma_{\Delta v}$	0.5	$\tilde{\gamma}$	0.51

### A. Full autonomous platoon scenario

We consider a platoon of  $N + 1 = 31$  autonomous vehicles, with desired inter-vehicular distance of  $\Delta \bar{p} = 20$  m. The controller parameters are described in Table I, and are chosen such that  $\tilde{\gamma} \approx 0.5$ . Figures 2a, 2b and 2c show, respectively, the inter-vehicular distance ( $-\Delta p_i$ ), speed tracking error ( $-\Delta v_i$ ) and the macroscopic variable ( $\rho_i^M$ ). The red line in Figure 2b represents the speed difference of vehicle  $i = 0$  with respect to the reference value. The simulation time is 60 seconds and is split into three main phases:

- 1)  $t \in [0, 15]$  s: the vehicles start with perturbed initial conditions, randomly generated in a neighbourhood of the equilibrium point. This means that  $\mu_{\Delta p,i} \neq -\Delta \bar{p}$ ,  $\mu_{\Delta v,i} \neq 0$  and  $\sigma_{\Delta p,i}^2, \sigma_{\Delta v,i}^2 \neq 0$ . In this phase the desired speed of vehicle  $i = 0$  is  $\bar{v}_1 = 20$  m/s.

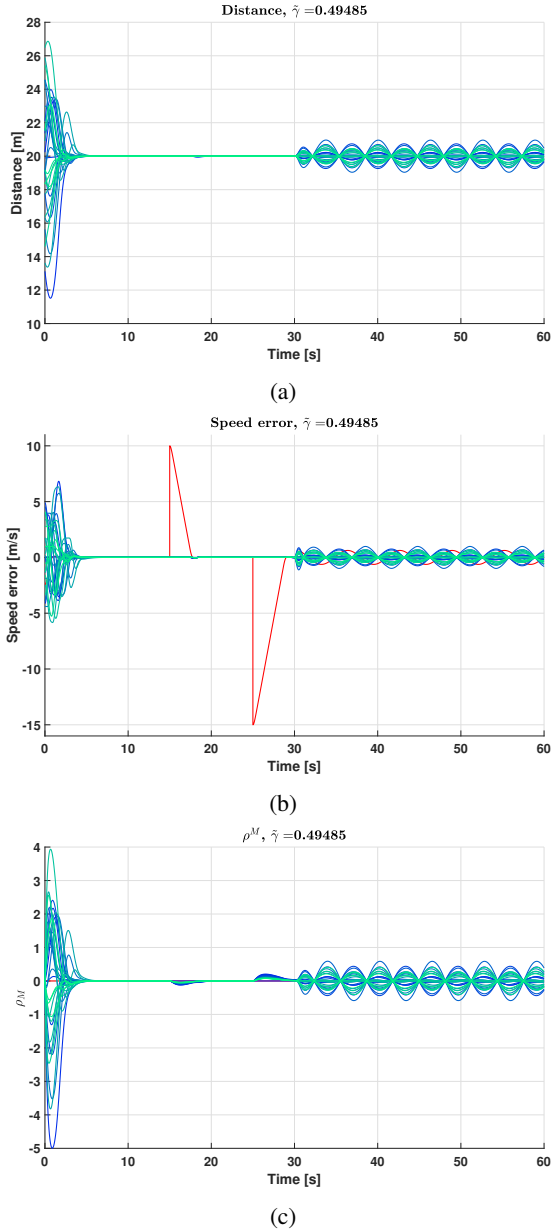


Fig. 2: Full autonomous platoon scenario. See Section V for the description and the color legend.

- 2)  $t \in [15, 30]$  s: vehicle  $i = 0$  tracks a variable reference speed. At 15 s, it accelerates from  $\bar{v}_1 = 20$  m/s to  $\bar{v}_2 = 30$  m/s; then, at 25 s it decelerates to  $\bar{v}_3 = 15$  m/s.
- 3)  $t \in [30, 60]$  s: the reference speed is 15 m/s. In this phase a sinusoidal disturbance  $d_i = r_i \sin(t)$  acts on each vehicle of the platoon, where  $r_i$  is a random number in the interval  $[-3, 3]$ .

In the first phase, the vehicles are able to converge to the desired speed and inter-vehicular distance. Both inter-vehicular distance and speed error trajectories result bounded during the transient interval that at about 5 s is already ended (see Figures 2a and 2b). In Figure 2c, we observe that the high perturbation due to the initial conditions is captured by the macroscopic function, showing marked overshoots. This causes the vehicles to track a variable reference distance, leading to the harmo-

nization of the transient phase. We observe that the disturbance due to the input delay does not affect the stability of the string. In the second phase, the leader vehicle is able to perfectly track the reference speed variation (see the red line in Figure 2b). The rest of the platoon is able to track vehicle  $i = 0$  without showing any propagating oscillations, specially at 15 s and 25 s where high amplitude peaks are generated by the step variation of the reference speed. Also, the vehicles successfully track the desired distance of  $\Delta \bar{p} = 20$  m (see Figure 2a). As in the first phase, no external disturbances in addition to the unmodeled input lag act on the platoon; then the data shared by each vehicle is correct and string stability is maintained. This high degree of reliability is caught by the macroscopic function, as it does not show high variations. Then, the desired distance for each vehicle remains close to the value of 20 m. In the third phase, a sinusoidal disturbance of amplitude  $r_i$ , with  $r_i$  taking random value in the interval  $[-3, 3]$ , corrupts the acceleration of each vehicle. Consequently, the control input does not match the real acceleration, meaning that the vehicles are sharing a corrupted information, and without a proper action the oscillations could amplify through the string. Despite the disturbances acting on the platoon, the sharing of the macroscopic information allow the system to have bounded trajectories. This means that the effects of the disturbances acting on the head of the platoon have a minor influence on the tail vehicles (see Figures 2a and 2b). In this phase, we observe that the macroscopic function shows sinusoidal trajectories, meaning that is catching the information about the existence of the acting disturbances. Then, each leader-follower pair can anticipate its action by properly varying the inter-vehicular distance. A filtering behavior of the perturbation arriving from ahead is observed, avoiding the amplification of the disturbances along the platoon, and then the disruption of the platoon itself.

### B. Mixed traffic scenario

We consider a string of  $N + 1 = 31$  both autonomous and human-driven vehicles, representing a mixed traffic scenario. The desired distance for the autonomous vehicles is  $\Delta \bar{p} = 20$  m and the controller parameters are reported in Table II. As before, the interconnection term is  $\tilde{\gamma} \approx 0.5$ . Differently from the first case, we set the weight corresponding to the speed difference macroscopic function  $\psi_{\Delta v}^i$  to zero ( $b = 0$ ), that resembles the more real situation in which the macroscopic information is shared by the infrastructure, that directly measures the traffic density here represented by the inter-vehicular distance mean  $\mu_{\Delta p, i}$  and variance  $\sigma_{\Delta p, i}^2$ . This means that the autonomous vehicles have information also of the non-autonomous ones. To the authors point of view, the proposed approach is consistent with the state-of-the-art technology. The dynamics of the human driven vehicles are modeled according to the Optimal Velocity model and the parameters in [31]. Each human driver follows a variable spacing policy with respect to the current speed, such that below a minimum safety distance, set to 5 m, the vehicle stops and above a maximum distance, set to 35 m, the vehicle maintains the maximum speed. We denote with  $\mathcal{I}_{HD} = \{4, 5, 13, 14, 15, 16\}$  the set of non autonomous vehicles. The inter-vehicular distance

$(-\Delta p_i)$ , speed tracking error  $(-\Delta v_i)$  and the macroscopic variable  $(\rho_i^M)$  are shown, respectively, in Figures 3a, 3b and 3d. The red line in Figure 3b represents the speed difference of vehicle  $i = 0$  with respect to the reference value. The  $\rho_i^M$  trajectories in Figure 3d refer only to the autonomous vehicles. Furthermore, to better appreciate the behavior of the mixed platoon, we report the vehicles speed in Figure 3c. In order to distinguish the human driven vehicles, trajectories  $j = 4, 5$  are represented by the purple scale and trajectories  $j = 13, 14, 15, 16$  are represented by the gray scale, as before from the light tint to the darker one. The simulation time is 80 seconds and is split into three phases:

- 1)  $t \in [0, 20]$  s: all the vehicles start in a normal traffic situation, with distance of 20 m and with speed corresponding to the desired value  $\bar{v}_1 = 19.4$  m/s.
- 2)  $t \in [20, 40]$  s: the platoon is forced to slow down to a speed of  $\bar{v}_2 = 11.1$  m/s, due to the presence of a bottleneck.
- 3)  $t \in [40, 80]$  s: after having surpassed the bottleneck, the platoon accelerates to  $\bar{v}_3 = 30.5$  m/s.

In the first phase, the autonomous vehicles are at the desired distance and speed. On the contrary, according with their variable spacing policy, the human driven vehicles are subject to a transient phase in which they reach the equilibrium distance of about 19.7 m (Figure 3a, gray trajectories). Since the human driven vehicles do not communicate any data, their adjustments are an unexpected behavior giving rise to perturbations in the string. In this phase, the autonomous vehicles are able to dissipate the perturbations deriving from the vehicles ahead, without showing any marked variations (see Figure 3b). In Figure 3d, we observe that the macroscopic function  $\rho_i^M$  with respect to the vehicles following the human driven ones is not zero, meaning that it successfully captures the information about the current state of the platoon. In the second and third phases, the leader vehicle firstly decelerates to 11.1 m/s and then it accelerates to 30.5 m/s. As a consequence, the non autonomous vehicles vary their inter-vehicular distances according to their spacing policy: in the decreasing speed phase they reduce their distance to 15.6 m, in the increasing speed phase they enlarge their distance to 25.3 m (Figure 3a). In order to counteract this behavior, that gives birth to disturbances inside the string, in the second phase ( $t \in [20, 40]$  s) the follower autonomous vehicles increase their distances. The macroscopic function  $\rho_i^M$  (Figure 3d) extracts the information embedded in the inter-vehicular distance mean  $\mu_{\Delta p, i}$  and variance  $\sigma_{\Delta p, i}^2$ , and let the autonomous vehicles to notice that the platoon state is away from the desired equilibrium point. Then, in order to be able to absorb possible perturbations arriving from ahead, they increase the distance. On the contrary, in the third phase, when the higher speed leads the non autonomous vehicles to increase their distances, the autonomous ones come closer in order to increase the traffic throughput. In Figure 3b it is shown the speed difference trajectories of the platoon. We observe that at 20 s and 30 s, the beginning of the second and third phases, the perturbation due to the step variation of the speed reference is correctly attenuated by the platoon. Moreover, also the oscillations

corresponding to the human driven vehicles (grey lines) do not amplify through the string, confirming the system to be disturbance string stable. In Figure 3c, we observe the same filtering action, where the speed of the autonomous vehicles following the non autonomous ones show a dampening of the oscillations.

### C. Traffic lights scenario

In this section, the simulations about a urban road scenario are reported. We consider a platoon of  $N+1 = 11$  autonomous vehicles moving in an urban area. More precisely, we analyze the case in which the vehicles are waiting at a traffic light. In Table III are reported the controller parameters, that are chosen such that  $\tilde{\gamma} \approx 0.5$  as in the other cases. Since in a urban area the velocities are lower, in this case we modified the control parameters in order to take into account the particular situation. Moreover, it is possible to exploit both V2V and V2I technologies. Then, the infrastructure, here represented by the traffic light, can communicate with the platoon and send traffic data in real-time, for example the light phases and the desired, or optimal, speed to cross the city road segments. Also in this case, we split the simulation into three main phases:

- 1)  $t \in [0, 10]$  s: the vehicles are waiting at the traffic light.
- 2)  $t \in [10, 45]$  s: the green light turn on and the first vehicle reach the speed of 8.3 m/s tracking a ramp reference signal.
- 3)  $t \in [45, 60]$  s: the platoon meets a red light, then it stops following a ramp reference signal.

We suppose that during the waiting phase the vehicles in the platoon have a small desired distance of  $\Delta \bar{p}_1 = 1$  m, while when moving they reach a larger reference distance of  $\Delta \bar{p}_2 = 2$  m in order to guarantee greater safety. Then, in order to avoid discontinuities, in the transition phases the vehicles are commanded to track a ramp desired distance with limited derivative, that connects the two desired values. Figures 4a, 4b and 4c refer to the distance  $(-\Delta p_i)$ , speed difference  $(-\Delta v_i)$  and the macroscopic function  $(\rho_i^M)$  with respect to the autonomous vehicles, respectively. The red line in Figure 4b represents the speed difference of the first vehicle with respect to the reference value.

In Figure 4a, we observe that the platoon correctly track the variable desired distance between  $[10, 15]$  s and  $[40, 45]$  s. More precisely, thanks to the accumulated macroscopic information the tail vehicles intensify their acceleration and anticipate their actions. This behavior allows the platoon to stay compact despite of the actuation delay. Indeed, we observe the green trajectory (the last vehicle) to converge faster to 2 m with respect to the other vehicles, except for the first one (blue line). In Figure 4b, we notice that the tracking of the variable speed reference does not generate perturbations in the string, letting the platoon be stable. The simulation results show that the proposed approach can be employed also in an urban scenario, allowing the control of platoons that have to meet tighter requirements dictated by the particular scenario.

## VI. CONCLUSIONS

In this paper, the possibility to exploit macroscopic information for ensuring vehicular platoon Disturbance String Stability

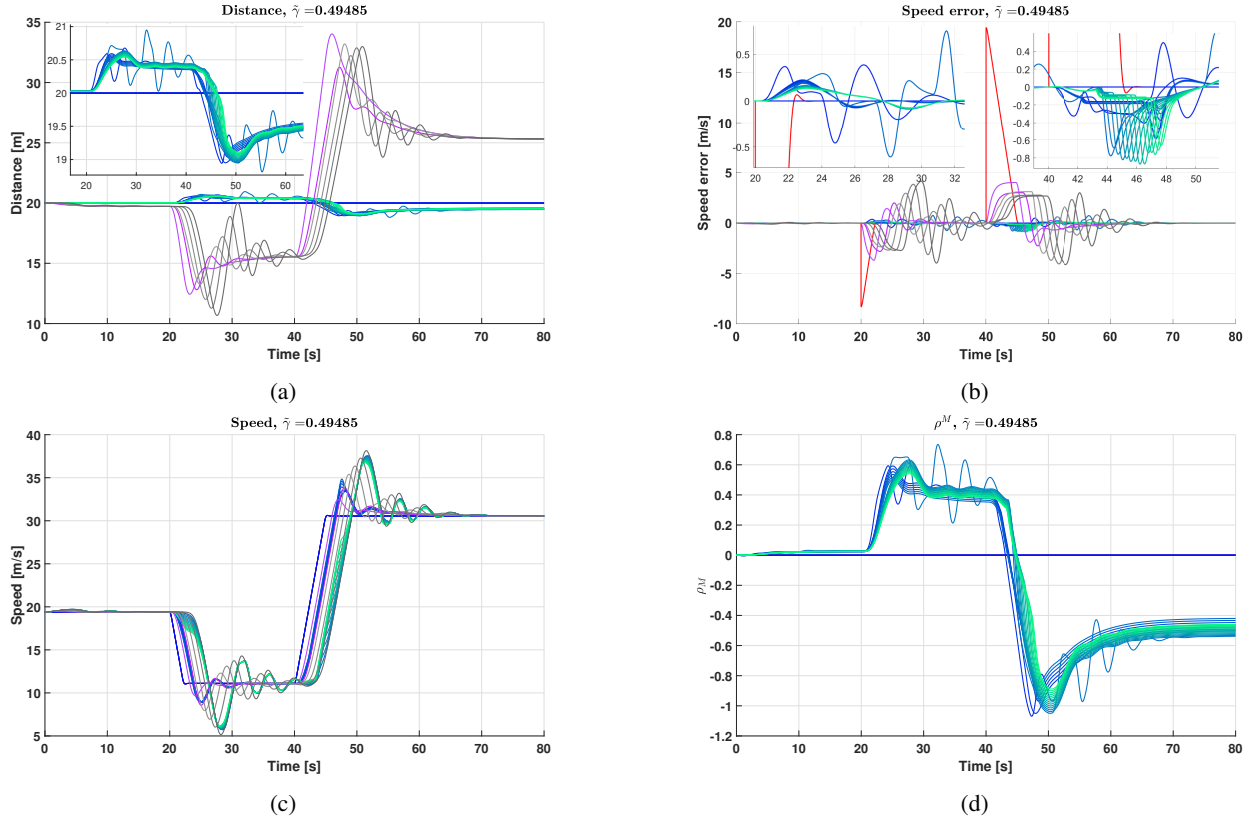


Fig. 3: Mixed traffic scenario. See Section V for the description and the color legend.

is investigated, and a rigorous stability analysis is provided. Disturbance String Stability is first proved for general systems having a cascaded interconnected structure, by using ISS concepts. Then, the result is applied to a platoon of autonomous vehicles subject to external disturbances. We show how the propagation of few variables embedding global information about the platoon ensures a proper response of the vehicles. Moreover, we illustrate how the same framework can be exploited to ensure the stability in the mixed traffic scenario, where non autonomous vehicles are present. A mesoscopic control law has been proposed, and the improvements due to the utilisation of macroscopic information are shown by means of simulations. To test the robustness of the proposed approach, three different scenarios have been tested in simulation: the first scenario refers to the case of a full autonomous platoon tracking a variable speed reference and subject to external disturbances, in the second scenario, the platoon is considered composed by both autonomous and human-driven vehicles, while the third scenario refers to the platoon starting from a traffic light and stopping to the next one. Therefore, the suggested approach is shown to be of interest for both urban and extra urban scenarios. The proposed results show that sharing macroscopic variables allows each vehicle to anticipate the needed control action and filter the perturbations acting on the ahead vehicles, thereby avoiding a disruptive amplification, and matching string stability requirements. Future work will focus on extending the proposed framework to more complex cases, by explicitly including the presence of communication delays. Also, different methods for the estimation of the

macroscopic variables will be investigated, and more realistic scenarios will be tested with the use of dedicated traffic simulators.

#### REFERENCES

- [1] J. Guanetti, Y. Kim, and F. Borrelli, “Control of connected and automated vehicles: State of the art and future challenges,” *Annual Reviews in Control*, vol. 45, pp. 18 – 40, 2018.
- [2] A. Talebpour and H. S. Mahmassani, “Influence of connected and autonomous vehicles on traffic flow stability and throughput,” *Transportation Research Part C: Emerging Technologies*, vol. 71, pp. 143 – 163, 2016.
- [3] V. Giammarino, S. Baldi, P. Frasca, and M. Delle Monache, “Traffic flow on a ring with a single autonomous vehicle: An interconnected stability perspective,” *IEEE Transactions On Intelligent Transportation Systems*, pp. 1–11, April 2020.
- [4] N. Mehr and R. Horowitz, “How will the presence of autonomous vehicles affect the equilibrium state of traffic networks?” *IEEE Transactions on Control of Network Systems*, vol. 7, no. 1, pp. 96–105, 2020.
- [5] A. Hegyi, Bart De Schutter, and J. Hellendoorn, “Optimal coordination of variable speed limits to suppress shock waves,” *IEEE Transactions on Intelligent Transportation Systems*, vol. 6, no. 1, pp. 102–112, 2005.
- [6] E. Uhlemann, “The US and Europe Advances V2V Deployment [Connected Vehicles],” *IEEE Vehicular Technology Magazine*, vol. 12, no. 2, pp. 18–22, June 2017.
- [7] S. Feng, Y. Zhang, S. E. Li, Z. Cao, H. X. Liu, and L. Li, “String stability for vehicular platoon control: Definitions and analysis methods,” *Annual Reviews in Control*, vol. 47, pp. 81–97, March 2019.
- [8] P. Caravani, E. De Santis, F. Graziosi, and E. Panizzi, “Communication control and driving assistance to a platoon of vehicles in heavy traffic and scarce visibility,” *IEEE Transactions on Intelligent Transportation Systems*, vol. 7, no. 4, pp. 448–460, Dec 2006.
- [9] D. Swaroop and J. K. Hedrick, “String stability of interconnected systems,” *IEEE Transactions on Automatic Control*, vol. 41, no. 3, pp. 349–357, Mar 1996.
- [10] M. Mirabilio, A. Iovine, E. De Santis, M. D. Di Benedetto, and G. Pola, “On the utilization of macroscopic information for string stability of a vehicular platoon,” in *2020 59th IEEE Conference on Decision and Control (CDC)*, 2020, pp. 2811–2816.

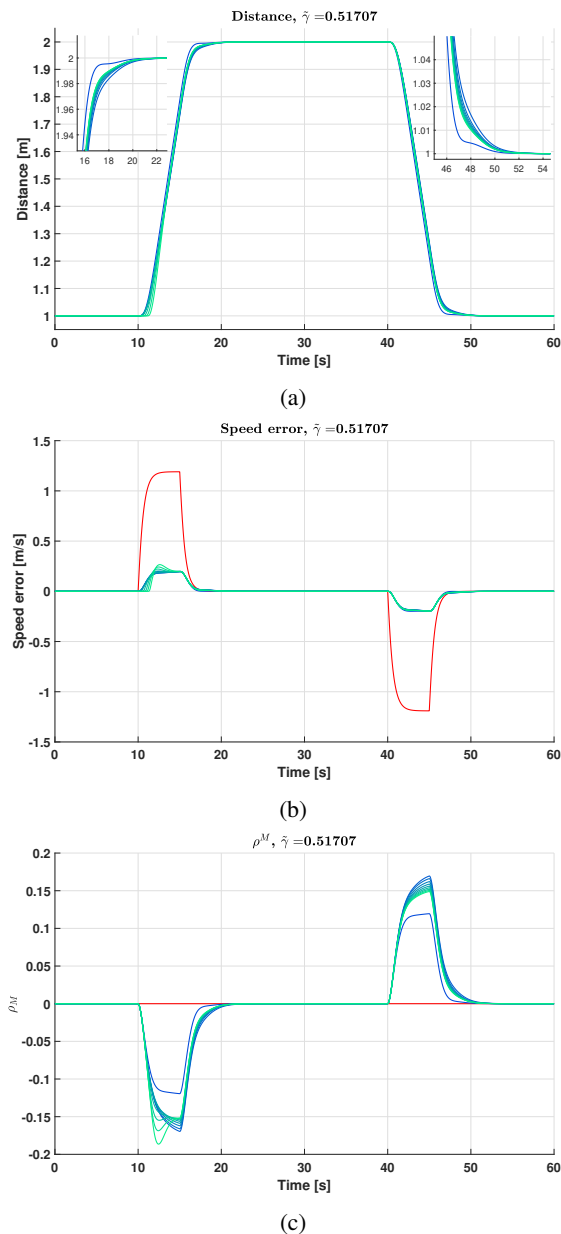


Fig. 4: Traffic lights scenario. See Section V for the description and the color legend.

- [11] M. Mirabilio, A. Iovine, E. De Santis, M. D. Di Benedetto, and G. Pola, "String stability of a vehicular platoon with the use of macroscopic information," *IEEE Transactions on Intelligent Transportation Systems*, vol. 22, no. 9, pp. 5861–5873, 2021.
- [12] R. Florin and S. Olariu, "Towards real-time density estimation using vehicle-to-vehicle communications," *Transportation Research Part B: Methodological*, vol. 138, pp. 435–456, 2020.
- [13] C. Wang, B. Ran, H. Yang, J. Zhang, and X. Qu, "A novel approach to estimate freeway traffic state: Parallel computing and improved kalman filter," *IEEE Intelligent Transportation Systems Magazine*, vol. 10, no. 2, pp. 180–193, 2018.
- [14] D. Swaroop and J. Hedrick, "Constant spacing strategies for platooning in automated highway systems," *Journal of Dynamic Systems Measurement and Control*, vol. 121, no. 3, September 1999.
- [15] B. Besselink and K. H. Johansson, "String stability and a delay-based spacing policy for vehicle platoons subject to disturbances," *IEEE Transactions on Automatic Control*, vol. 62, no. 9, pp. 4376–4391, March 2017.
- [16] M. Treiber and A. Kesting, *Traffic flows dynamics*. Springer, 2013.
- [17] A. Jamshidnejad, I. Papamichail, M. Papageorgiou, and B. De Schutter, "A mesoscopic integrated urban traffic flow-emission model," *Transportation Research Part C: Emerging Technologies*, vol. 75, pp. 45 –

83, 2017.

- [18] D. Swaroop and R. Huandra, "Intelligent cruise control system design based on a traffic flow specification," *Vehicle System Dynamics: International Journal of Vehicle Mechanics and Mobility*, vol. 30, no. 5, pp. 319–344, November 1998.
- [19] S. Darbha and K. Rajagopal, "Intelligent cruise control systems and traffic flow stability," *Transportation Research Part C: Emerging Technologies*, vol. 7, no. 6, pp. 329–352, 1999.
- [20] A. Iovine, F. Valentini, E. De Santis, M. D. Di Benedetto, and M. Pratesi, "Safe human-inspired mesoscopic hybrid automaton for autonomous vehicles," *Nonlinear Analysis: Hybrid Systems*, vol. 25, pp. 192 – 210, 2017.
- [21] A. Ibrahim, M. Čičić, D. Goswami, T. Basten, and K. Johansson, "Control of platooned vehicles in presence of traffic shock waves," *IEEE Intelligent Transportation Systems Conference (ITSC)*, pp. 1727–1734, 2019.
- [22] H. K. Khalil, *Nonlinear systems*. Prentice Hall, 2002.
- [23] C. M. Kellett, "A compendium of comparison function results," *Mathematics of Control, Signals, and Systems*, vol. 26, no. 3, pp. 339–374, 2014.
- [24] L. Xiao and F. Gao, "Practical string stability of platoon of adaptive cruise control vehicles," *IEEE Transactions on Intelligent Transportation Systems*, vol. 12, no. 4, pp. 1184–1194, Dec 2011.
- [25] M. di Bernardo, A. Salvi, and S. Santini, "Distributed consensus strategy for platooning of vehicles in the presence of time-varying heterogeneous communication delays," *IEEE Transactions on Intelligent Transportation Systems*, vol. 16, no. 1, pp. 102–112, 2015.
- [26] V. K. Vegamoor, S. Darbha, and K. R. Rajagopal, "A review of automatic vehicle following systems," *Journal of the Indian Institute of Science*, vol. 99, p. 567 – 587, 2019.
- [27] J. Ploeg, N. van de Wouw, and H. Nijmeijer, " $\mathcal{L}_p$  string stability of cascaded systems application to vehicle platooning," *IEEE Transactions on Control Systems Technology*, vol. 22, no. 2, pp. 786–793, March 2014.
- [28] Y. Zheng, S. Ebel Li, K. Li, F. Borrelli, and J. Hedrick, "Distributed model predictive control for heterogeneous vehicle platoons under unidirectional topologies," *IEEE Transactions on Control Systems Technology*, vol. 25, no. 3, pp. 899–910, May 2017.
- [29] P. Seiler, A. Pant, and K. Hedrick, "Disturbance propagation in vehicle strings," *IEEE Transactions on Automatic Control*, vol. 49, no. 10, pp. 1835–1842, Oct 2004.
- [30] A. Ferrara, S. Sacone, and S. Siri, *Microscopic and Mesoscopic Traffic Models*. Cham: Springer International Publishing, 2018, pp. 113–143. [Online]. Available: [https://doi.org/10.1007/978-3-319-75961-6\\_5](https://doi.org/10.1007/978-3-319-75961-6_5)
- [31] J. I. Ge and G. Orosz, "Optimal control of connected vehicle systems with communication delay and driver reaction time," *IEEE Transactions on Intelligent Transportation Systems*, vol. 18, no. 8, pp. 2056–2070, 2017.
- [32] J. I. Ge, "Connected cruise control design in mixed traffic flow consisting of human-driven and automated vehicles," Ph.D. dissertation, University of Michigan, 2017.
- [33] R. E. Stern, S. Cui, M. L. Delle Monache, R. Bhadani, M. Bunting, M. Churchill, N. Hamilton, R. Haulcy, H. Pohlmann, F. Wu, B. Piccoli, B. Seibold, J. Sprinkle, and D. B. Work, "Dissipation of stop-and-go waves via control of autonomous vehicles: Field experiments," *Transportation Research Part C: Emerging Technologies*, vol. 89, pp. 205 – 221, 2018.
- [34] Y. Sugiyama, M. Fukui, M. Kikuchi, K. Hasebe, A. Nakayama, K. Nishinari, S. ichi Tadaki, and S. Yukawa, "Traffic jams without bottlenecks—experimental evidence for the physical mechanism of the formation of a jam," *New Journal of Physics*, vol. 10, no. 3, p. 033001, mar 2008.
- [35] S. ichi Tadaki, M. Kikuchi, M. Fukui, A. Nakayama, K. Nishinari, A. Shibata, Y. Sugiyama, T. Yosida, and S. Yukawa, "Phase transition in traffic jam experiment on a circuit," *New Journal of Physics*, vol. 15, no. 10, p. 103034, oct 2013.
- [36] V. Giammarino, M. Lv, S. Baldi, P. Frasca, and M. L. Delle Monache, "On a weaker notion of ring stability for mixed traffic with human-driven and autonomous vehicles," in *2019 IEEE 58th Conference on Decision and Control (CDC)*, 2019, pp. 335–340.
- [37] Z. P. Jiang, A. R. Teel, and L. Praly, "Small-gain theorem for ISS systems and applications," *Mathematics of Control, Signals, and Systems*, vol. 7, no. 2, pp. 95–120, 1994.

## APPENDIX

## A. Proof of Theorem 1

The proof of the Asymptotic String Stability for the nominal case with  $\bar{d}_i = 0$ ,  $\forall i \in \mathcal{I}_N^0$ , has already been provided in [10] for a specific case and generalized in [11]. These results are extended in the sequel to the case with disturbances. The first step is to obtain a common bound for all trajectories  $\tilde{\chi}_i(t)$  valid for all  $t \geq t_0$ , then an estimation of (13) is proven to exist. Since the assumption  $\gamma(s) \leq \tilde{\gamma}s$  holds, and  $\sigma \in \mathcal{K}_\infty$  implies  $\sigma(|\bar{d}_i(\cdot)|_\infty^{[0,t]}) \leq \sigma(\max_{i \in \mathcal{I}_N^0} |\bar{d}_i(\cdot)|_\infty^{[0,t]})$ , inequality

$$\max_{i \in \mathcal{I}_N^0} |\tilde{\chi}_i(t)| \leq \frac{1}{1-\tilde{\gamma}} \beta \left( \max_{i \in \mathcal{I}_N^0} |\tilde{\chi}_i(0)|, 0 \right) + \frac{1}{1-\tilde{\gamma}} \sigma \left( \max_{i \in \mathcal{I}_N^0} |\bar{d}_i(\cdot)|_\infty^{[0,t]} \right), \quad \forall t \geq 0. \quad (26)$$

can be proven by applying the same forward recursive method shown in [11, Theorem 1]. By definition of class  $\mathcal{K}_\infty$  and  $\mathcal{K}\mathcal{L}$  functions,  $\beta$  and  $\sigma$  are invertible; then, for  $\tilde{\gamma} \in (0, 1)$  and for any  $\epsilon > 0$ , there exist at least a pair  $\delta, \delta_d$  such that

$$\beta(\delta, 0) + \sigma(\delta_d) = (1 - \tilde{\gamma})\epsilon < \epsilon. \quad (27)$$

If  $|\tilde{\chi}(0)|_\infty \leq \delta$  and  $\max_{i \in \mathcal{I}_N^0} |\bar{d}_i(\cdot)|_\infty^{[0,t]} \leq \delta_d$ , then  $\max_{i \in \mathcal{I}_N^0} |\tilde{\chi}_i(\cdot)|_\infty^{[0,t]} < \epsilon$ . Now we can proceed by proving that an estimation of (13) exists. Let us introduce  $\hat{\beta}_0 = \frac{1}{1-\tilde{\gamma}} \beta(r, 0)$ ,  $\hat{\sigma}(s) = \frac{1}{1-\tilde{\gamma}} \sigma(s)$ ,  $r, s \geq 0$ ,  $\bar{d}_\infty^{[t_1, t_2]} = \max_{i \in \mathcal{I}_N^0} |\bar{d}_i(\cdot)|_\infty^{[t_1, t_2]}$ , and  $\mu = \hat{\beta}_0(|\tilde{\chi}(0)|_\infty) + \hat{\sigma}(\bar{d}_\infty^{[0,t]})$ . We recall that the ISS inequality (15) can be computed with respect to a general initial time instant  $\tau \in [0, t]$ . Then, we get:

$$|\tilde{\chi}_i(t)| \leq \beta(|\tilde{\chi}_i(\tau)|, t - \tau) + \tilde{\gamma} \max_{j=0, \dots, i-1} |\tilde{\chi}_j(\cdot)|_\infty^{[\tau, t]} + \sigma \left( \bar{d}_\infty^{[\tau, t]} \right). \quad (28)$$

We recall that  $\sigma \in \mathcal{K}_\infty$  implies  $\sigma \left( \bar{d}_\infty^{[\tau, t]} \right) \leq \sigma \left( \bar{d}_\infty^{[0, t]} \right)$ . By exploiting (26) and choosing  $\tau = t/2$  in (28), for  $i = 0$  we get:

$$\begin{aligned} |\tilde{\chi}_0(t)| &\leq \beta(|\tilde{\chi}_0(t/2)|, t/2) + \sigma \left( \bar{d}_\infty^{[0, t]} \right) \\ &\leq \beta(\mu, t/2) + \sigma \left( \bar{d}_\infty^{[0, t]} \right). \end{aligned} \quad (29)$$

For  $i = 1$ , we get:

$$|\tilde{\chi}_1(t)| \leq \beta(|\tilde{\chi}_1(t/2)|, t/2) + \tilde{\gamma} |\tilde{\chi}_0(\cdot)|_\infty^{[t/2, t]} + \sigma \left( \bar{d}_\infty^{[0, t]} \right). \quad (30)$$

Since  $g_{cl}(\tilde{\chi}_{-1}) = 0$ , by definition of  $\mu$ , and using inequality (28), for  $i = 0$

$$|\tilde{\chi}_0(\cdot)|_\infty^{[t/2, t]} \leq \beta(\mu, t/4) + \sigma \left( \bar{d}_\infty^{[0, t]} \right) \quad (31)$$

holds. Recurring again to the definition of  $\mu$ , using (31) in (30) we get:

$$|\tilde{\chi}_1(t)| \leq \beta(\mu, t/2) + \tilde{\gamma} \beta(\mu, t/4) + (1 + \tilde{\gamma}) \sigma \left( \bar{d}_\infty^{[0, t]} \right). \quad (32)$$

By following the same procedure, for  $i = 2$  we obtain:

$$\begin{aligned} |\tilde{\chi}_2(t)| &\leq \beta(|\tilde{\chi}_2(t/2)|, t/2) + \sigma \left( \bar{d}_\infty^{[0, t]} \right) \\ &\quad + \tilde{\gamma} \max_{j=0, 1} |\tilde{\chi}_j(\cdot)|_\infty^{[t/2, t]}. \end{aligned} \quad (33)$$

From (32), we get

$$|\tilde{\chi}_1(t)|_\infty^{[t/2, t]} \leq \beta(\mu, t/4) + \tilde{\gamma} \beta(\mu, t/8) + (1 + \tilde{\gamma}) \sigma \left( \bar{d}_\infty^{[0, t]} \right). \quad (34)$$

Since the assumption  $\tilde{\gamma} \in (0, 1)$  and the definition of class  $\mathcal{K}\mathcal{L}$  function, then (34) holds also for  $i = 0$ . Then, for  $i = 2$  we get:

$$|\tilde{\chi}_2(t)| \leq \sum_{k=0}^2 \tilde{\gamma}^k \left( \beta \left( \mu, \frac{t}{2^{k+1}} \right) + \sigma \left( \bar{d}_\infty^{[0, t]} \right) \right). \quad (35)$$

By repeating the same procedure for each  $i \in \mathcal{I}_N^0$  we get:

$$|\tilde{\chi}_i(t)| \leq \sum_{k=0}^i \tilde{\gamma}^k \left( \beta \left( \mu, \frac{t}{2^{k+1}} \right) + \sigma \left( \bar{d}_\infty^{[0, t]} \right) \right). \quad (36)$$

As in [15], we define the  $\mathcal{K}\mathcal{L}$  function  $\phi(r, s) = \sup_{\omega \in (0, 1]} \omega^q \beta(r, \omega s)$ , for some  $q > 0$ . By multiplying and dividing  $\beta$  in (36) for  $(1/2^{k+1})^q$ , we get:

$$|\tilde{\chi}_i(t)| \leq \sum_{k=0}^i \left( 2^q (2^q \tilde{\gamma})^k \phi(\mu, t) + \tilde{\gamma}^k \sigma \left( \bar{d}_\infty^{[0, t]} \right) \right). \quad (37)$$

If parameter  $q$  is chosen such that  $\tilde{\gamma} < 2^{-q} < 1$ , then

$$|\tilde{\chi}_i(t)| \leq \frac{1}{2^{-q} - \tilde{\gamma}} \phi(\mu, t) + \hat{\sigma} \left( \bar{d}_\infty^{[0, t]} \right). \quad (38)$$

Let us define  $\bar{\beta}(r, s) = \phi(r, s) / (2^{-q} - \tilde{\gamma})$ . Since  $\mu = \hat{\beta}_0(|\tilde{\chi}(0)|_\infty) + \hat{\sigma}(\bar{d}_\infty^{[0, t]})$ , in order to address the appearance of  $\hat{\sigma}(\bar{d}_\infty^{[0, t]})$  in the first argument of  $\bar{\beta}$  we introduce the following bound:

$$k(r, \hat{\sigma}(s), t) = \min \left\{ \bar{\beta}(\hat{\beta}_0(r) + \hat{\sigma}(s), t), \hat{\beta}_0(r) \right\}. \quad (39)$$

As shown in [37], for any  $\alpha \in \mathcal{K}_\infty$

$k(r, \hat{\sigma}(s), t - t_0) \leq \bar{\beta}(\hat{\beta}_0(r) + \alpha^{-1}(r), t - t_0) + \hat{\beta}_0 \circ \alpha(\hat{\sigma}(s))$ , that leads to

$$|\tilde{\chi}| \leq \beta_d(|\tilde{\chi}(0)|_\infty, t) + \sigma_d \left( \bar{d}_\infty^{[0, t]} \right), \quad \forall i \in \mathcal{I}_N^0, \quad (40)$$

where  $\beta_d(r, s) = \bar{\beta}(\hat{\beta}_0(r) + \alpha^{-1}(r), s) \in \mathcal{K}\mathcal{L}$  and  $\sigma_d(r) = \bar{\sigma}(r) + \hat{\beta}_0 \circ \alpha(\bar{\sigma}(r)) \in \mathcal{K}_\infty$ . Then, Disturbance String Stability of the cascaded interconnected system with dynamics (14) is proven.

## B. Proof of Theorem 2

By exploiting Lyapunov stability theory (see [22]), we prove that the system state trajectory evolution  $\tilde{\chi}_i$  for each  $i \in \mathcal{I}_N^0$  is bounded by (15). Let us consider the candidate Lyapunov function  $W(\tilde{\chi}_i)$  for the  $i$ -th dynamical system (20):

$$W(\tilde{\chi}_i) = \frac{1}{2} \tilde{\chi}_i^T P_W \tilde{\chi}_i, \quad (41)$$

with

$$P_W = \begin{bmatrix} 1 & 0 & 2 & 0 \\ 0 & 1 & -2\lambda_1 & 2 \\ 0 & 0 & 2 + \lambda_1^2 & 2\lambda_1 \\ 0 & 0 & 0 & 2 \end{bmatrix}.$$

In the sequel, we denote  $W_i = W(\tilde{\chi}_i)$ . Since  $P_W$  is an upper triangular square matrix, it is straightforward to compute the lower and the upper bound of  $W_i$  as two quadratic functions that depend, respectively, on the minimum and maximum eigenvalues of  $P$ :

$$\underline{\alpha}|\tilde{\chi}_i|^2 \leq W_i \leq \bar{\alpha}|\tilde{\chi}_i|^2, \quad (42)$$

where  $\underline{\alpha} = 1/2$  and  $\bar{\alpha} = (2 + \lambda_1^2)/2$ . We start the analysis for the nominal system, with no disturbances. The time derivative of  $W_i$  is:

$$\dot{W}_i = -\tilde{\chi}_i^T Q_W \tilde{\chi}_i + \rho_{2,i} \psi_{a,b}^{i-1} \quad (43)$$

with  $Q_W$  being an upper triangular square matrix:

$$Q_W = \begin{bmatrix} K_{\Delta p} & * & * & * \\ 0 & K_{\Delta v} & * & * \\ 0 & 0 & 2K_{\Delta p} + K_{\Delta v}\lambda_1^2 + \lambda_1 & * \\ 0 & 0 & 0 & K_{\Delta v} + \lambda_2 \end{bmatrix},$$

where we omit the terms out of the main diagonal since they are of no use in the calculation of the eigenvalues of  $Q_W$ . Since the assumption  $K_{\Delta p}, K_{\Delta v}, \lambda_1, \lambda_2 > 0$  holds, the minimum eigenvalue of  $Q_W$  is  $\alpha = \min\{K_{\Delta p}, K_{\Delta v}\}$ . Then,

$$\dot{W}_i \leq -\alpha|\tilde{\chi}_i|^2 + |\tilde{\chi}_i|\psi_{a,b}^{i-1}. \quad (44)$$

By exploiting mean and variance properties, the following inequality holds for  $\psi_{a,b}^i$  (see [10]):

$$|\psi_{a,b}^i| = a|\psi_{\Delta p}^i| + b|\psi_{\Delta v}^i| \leq (a\gamma_{\Delta p} + b\gamma_{\Delta v}) \max_{j=0,\dots,i} |\tilde{\chi}_j|. \quad (45)$$

Define  $\Upsilon \in (0, 1)$  and  $c_\psi = a\gamma_{\Delta p} + b\gamma_{\Delta v}$ ; then

$$\begin{aligned} \dot{W}_i &\leq -\alpha(1 - \Upsilon)|\tilde{\chi}_i|^2 + |\tilde{\chi}_i| \left( c_\psi \max_{j=0,\dots,i-1} |\tilde{\chi}_j| - \alpha\Upsilon|\tilde{\chi}_i| \right) \\ &\leq -\alpha(1 - \Upsilon)|\tilde{\chi}_i|^2, \quad \forall |\tilde{\chi}_i| \geq \frac{c_\psi}{\alpha\Upsilon} \max_{j=0,\dots,i-1} |\tilde{\chi}_j|. \end{aligned} \quad (46)$$

Since  $\alpha > 0$ , the inequality (46) satisfies the Input-to-State Stability (ISS) condition [22]. Therefore, for each  $i \in \mathcal{I}_N^0$ ,

$$|\tilde{\chi}_i| \leq \beta(|\tilde{\chi}_i(0)|, t) + \gamma \left( \max_{j=0,\dots,i-1} |\tilde{\chi}_j|_{\infty}^{[0,t]} \right), \quad \forall t \geq 0,$$

with

$$\gamma(s) = \tilde{\gamma}s \quad \forall s \geq 0, \quad \tilde{\gamma} = \sqrt{\frac{\bar{\alpha}}{\alpha}} \frac{c_\psi}{\alpha\Upsilon} > 0. \quad (47)$$

Since the parameters  $a, b \geq 0$  in (18) can be arbitrarily selected, the constant  $c_\psi$  can be chosen such that  $\tilde{\gamma} \in (0, 1)$ .

We now prove that the  $i$ -th system also verifies the ISS condition with respect to the disturbance  $\bar{d}_i$ . We define  $\alpha_{ss} = \alpha(1 - \Upsilon)$ . If the inequality on  $\tilde{\chi}_i$  in (46) is verified, then the following holds:

$$\begin{aligned} \dot{W}_i &\leq -\alpha_{ss}|\tilde{\chi}_i|^2 + |c_d|(\Delta v_i - \lambda_1\rho_{1,i-1} + \rho_{2,i-1})\bar{d}_i \\ &\leq -\alpha_{ss}|\tilde{\chi}_i|^2 + \underbrace{\sqrt{2}|c_d|\max\{1, \lambda_1\}}_{c'_d} |\tilde{\chi}_i|\bar{d}_i \\ &\leq -\alpha_{ss}|\tilde{\chi}_i|^2 + \frac{1}{2c}|\tilde{\chi}_i|^2 + \frac{c}{2}c_d'^2|\bar{d}_i|^2, \end{aligned} \quad (48)$$

where we exploited the inequality  $|xy| \leq \frac{1}{2c}x^2 + \frac{c}{2}y^2$ ,  $c > 0$ . By choosing  $c = 1/\alpha_{ss}$ , we get

$$\dot{W}_i \leq -\frac{\alpha_{ss}}{2}|\tilde{\chi}_i|^2 + \frac{c_d'^2}{2\alpha_{ss}}|\bar{d}_i|^2.$$

Then, the inequality in (15) is verified with  $\sigma(s) = \underline{\alpha}^{-1} \circ \bar{\alpha} \circ \alpha_{ss}^{-1} \circ 2\vartheta(s)$ , where

$$\vartheta(s) = \frac{c_d'^2}{2\alpha_{ss}}s^2, \quad (49)$$

and

$$\sigma(s) = \tilde{\sigma}s \quad \forall s \geq 0, \quad \tilde{\sigma} = \sqrt{\frac{2\bar{\alpha}}{\alpha}} \frac{c'_d}{\alpha_{ss}} > 0. \quad (50)$$

On the basis of Theorem 1, Disturbance String Stability of the platoon can be obtained by an appropriate tuning of the controller parameters.